



Mesoscopic approach to progressive breakdown in ultrathin Si O₂ layers

E. Miranda

Citation: [Applied Physics Letters](#) **91**, 053502 (2007); doi: 10.1063/1.2761831

View online: <http://dx.doi.org/10.1063/1.2761831>

View Table of Contents: <http://scitation.aip.org/content/aip/journal/apl/91/5?ver=pdfcov>

Published by the [AIP Publishing](#)



Re-register for Table of Content Alerts

Create a profile.



Sign up today!



Mesoscopic approach to progressive breakdown in ultrathin SiO₂ layers

E. Miranda^{a)}

Departament d'Enginyeria Electrònica, Universitat Autònoma de Barcelona, Edifici Q,
08193 Bellaterra, Spain

(Received 21 May 2007; accepted 28 June 2007; published online 31 July 2007)

The opening of a breakdown path across the ultrathin oxide layer in a metal-oxide-semiconductor structure caused by the application of electrical stress can be analyzed within the framework of the physics of mesoscopic conductors. Using the Landauer formula for a quantum point contact, the author is able to show that the saturation of the gate leakage current is linked to the progressive evolution of the constriction's conductance toward the ballistic transport regime. The possible physical mechanisms responsible for energy dissipation inside the breakdown path as well as the limitations of the proposed approach are discussed. © 2007 American Institute of Physics.

[DOI: 10.1063/1.2761831]

It is widely recognized that the application of electrical stress to an ultrathin dielectric in a metal-oxide-semiconductor (MOS) structure can open, following a degradation process in which traps or defects are randomly created across the oxide layer, a localized conducting path running between gate and substrate.¹ This is the signature of dielectric breakdown (BD). In relatively thick oxides, from 3 to 6 nm, this event is characterized by an abrupt change of conduction mechanism that leads to a bimodal post-BD current distribution. These stable conduction modes are often referred to as soft BD (SBD) and hard BD (HBD) and are presumably associated with preferred atomic configurations.² On the other hand, if the oxide thickness is less than 2 nm and the voltage applied to the gate is low enough, the current flowing through the broken down device exhibits an evolutionary behavior which reveals the progressive lateral enlargement of the leakage spot size.³ This transitory, also called progressive breakdown (PBD), ends when the system arrives to a final HBD state. Even though the issue has been extensively investigated, mainly from the oxide reliability viewpoint, there are still many dark points concerning the details of the electron transport process through this nanometer-sized constriction. To deal with this problem, a number of models based on mechanisms such as percolation in nonlinear conductor networks, variable range hopping, tunneling, and quantum-point contact (QPC) conduction among others have been proposed.⁴ In particular, the QPC model is able to explain consistently the shape of the I - V characteristics for both the SBD and HBD conduction modes. According to this model, the main distinction between SBD and HBD is the cross-sectional area of the constriction at its narrowest point. In mesoscopic devices, the transversal confinement induces energy subbands which act as potential barriers for the incoming electrons so that the conduction properties of the BD path are determined by the transmission probability coefficient.⁴ Here, we extend these concepts and show that the BD spot cannot be regarded as an isolated entity since factors such as the series resistance and background tunneling current must be taken into account to simulate properly the dynamical behavior of the whole system when subjected to stressing conditions. In this way, by

means of a separate analysis of the power dissipated at each part of the proposed equivalent circuit model, we are able to connect the local heating effects at the constriction's bottleneck with the current saturation.

For the experiments we used standard MOS capacitors with p -type Si substrate (10^{15} cm⁻³) and poly-Si gate. The nominal oxide thickness is 2.1 nm and the gate area is 6.4×10^{-5} cm². Figure 1 shows three experimental gate current-time (I_G - t) characteristics measured under accumulation conditions with a constant voltage stress $V_G = -3.75$ V. Notice that the outset of PBD is sample-to-sample dependent, as expected, and that the sigmoidal behavior is a common feature of all curves. In particular, curves C1 and C2 reach the same current level within the considered time window. Initial differences in the tunneling current, such as that exhibited by curve C3, may be attributed to oxide thickness variations. If we assume that I_G , at any moment, consists of the tunneling current contribution flowing through the non-

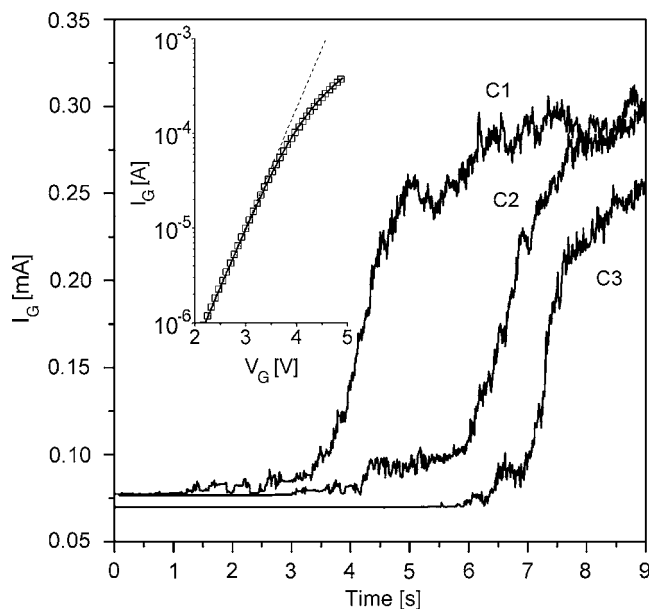


FIG. 1. Three experimental gate current-time characteristics obtained during a constant voltage stress at $V_G = -3.75$ V. The inset shows a typical fresh I_G - V_G characteristic (squares). The solid and dashed lines are obtained using the tunneling model considered in Eq. (1) with $R_S = 1.75$ k Ω and $R_S = 0$ k Ω , respectively. In both cases, $A = 2.16 \times 10^{-9}$ A and $B = 2.9$ V⁻¹.

^{a)}Electronic mail: enrique.miranda@uab.es

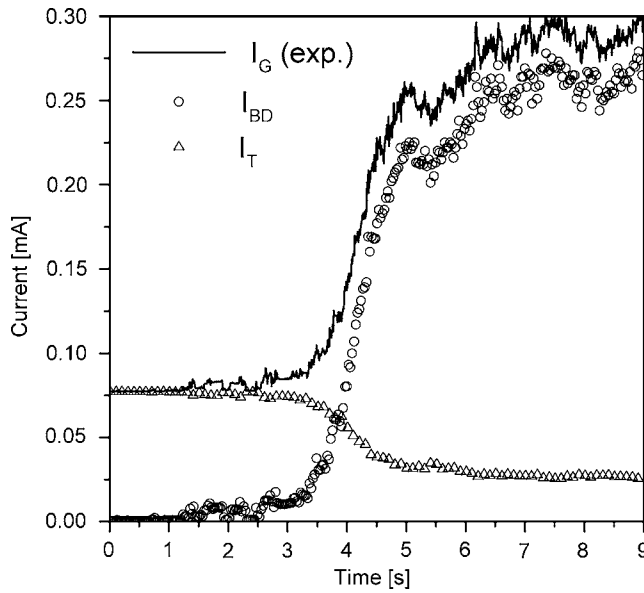


FIG. 2. Evolution of the total gate current I_G (solid line) and its two components calculated using Eq. (1): the tunneling current I_T (triangles) that flows distributed throughout the gate area and the local current I_{BD} (circles) that flows localized through the PBD path.

damaged area of the device I_T and the current flowing in parallel through the BD spot I_{BD} we can find the post-BD conductance G_{BD} as

$$G_{BD} = \frac{I_{BD}}{V_{ox}} = \frac{I_G - I_T}{V_{ox}} = \frac{I_G - A \exp[B(V_G - I_G R_S)]}{V_G - I_G R_S}, \quad (1)$$

where V_{ox} is the voltage drop across the oxide layer. Within this approach, the direct tunneling current is represented by a simple exponential function of V_{ox} whose parameters A and B are determined from the fresh I_G - V_G characteristic (see inset of Fig. 1). Of course, more elaborated models for I_T can be used but this is unnecessary for our aims. R_S is the series resistance extracted from the high-bias region of the fresh I_G - V_G curve. Eq. (1) is valid as long as the area of the PBD spot remains negligible compared with the total device area and the post-BD conductance is in the linear regime.⁴ Using the definitions of I_{BD} and I_T in Eq. (1), we can calculate separately both gate current components. These results are illustrated in Fig. 2 using the experimental data of curve C1. As a first consequence of this approach, notice that we have isolated the actual leakage current associated with the BD path. This is different from an earlier analysis in which the tunneling current preceding the detection of PBD was included as part of the logistic trajectory.⁵ Second, because of the potential drop across R_S , I_T decreases until reaching a lower steady state conduction level. Alternatively, we can analyze the behavior of the system in terms of power dissipation. At the outset, the dissipated power in the structure is mostly associated with the tunneling mechanism and dissipation takes place at the capacitor electrodes. On the contrary, after saturation, the power is mainly dissipated at the BD spot. A major point that needs to be investigated is how this latter power evolves and specifically where it is being dissipated. In what follows, we attempt to describe a plausible scenario based on the physics of mesoscopic conducting systems.

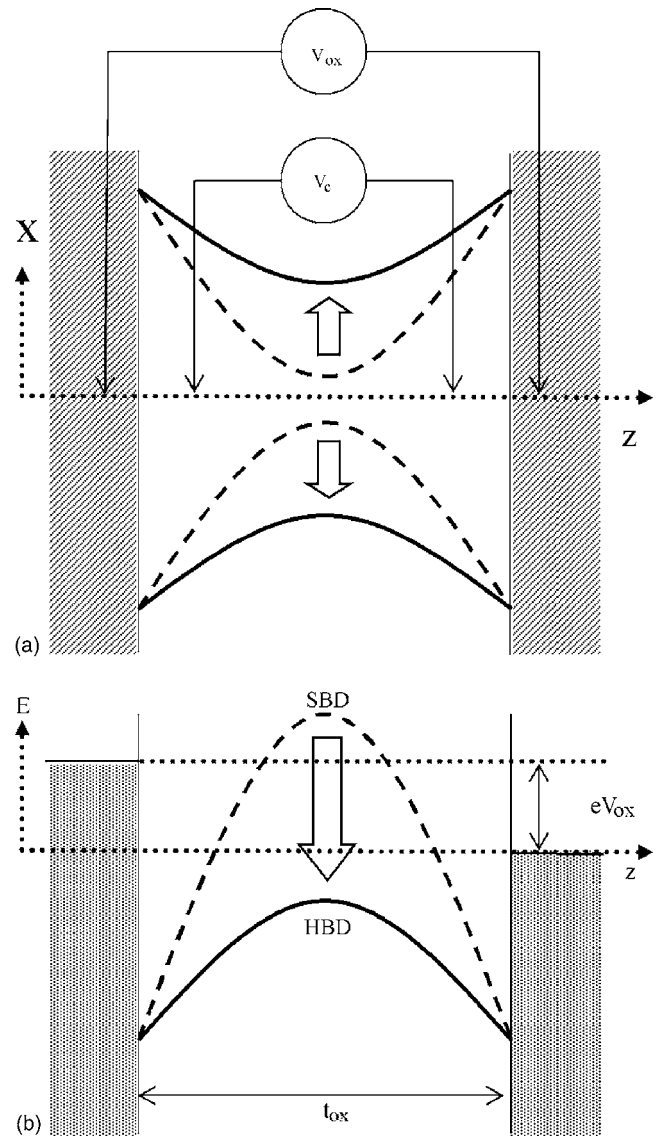


FIG. 3. (a) Schematic view of the breakdown path across the dielectric layer. The dashed line corresponds to the SBD conduction mode (lower current), whereas the solid line corresponds to the HBD mode (higher current). V_{ox} and V_c are the potential drops across the PBD path and across its narrowest point, respectively. (b) Energy diagram of the tunneling barrier associated with the transversal confinement. t_{ox} is the oxide thickness.

Using the Landauer formula for the conductance of a single-mode QPC, we calculate an average transmission probability \tilde{T} as⁶

$$\tilde{T} = G_0^{-1} G_{BD} = (G_0 V_{ox})^{-1} I_{BD}, \quad (2)$$

where $G_0 = 2e^2/h = (12.9 \text{ k}\Omega)^{-1}$ is the quantum conductance unit, e and h being the electron charge and Planck's constant, respectively. Even though Eq. (2) is strictly valid for very low biases in the zero-temperature limit, this oversimplification allows us to overlook the details of the confinement potential profile.⁷ The central point of our approach is that the power dissipated at the narrowest section of the constriction P_C is given by

$$P_C = I_{BD} V_c = (1 - \tilde{T}) I_{BD} V_{ox} = [1 - (G_0 V_{ox})^{-1} I_{BD}] I_{BD} V_{ox}, \quad (3)$$

where V_c is the voltage drop across the potential barrier associated with the first subband, as shown in Fig. 3(a). Notice

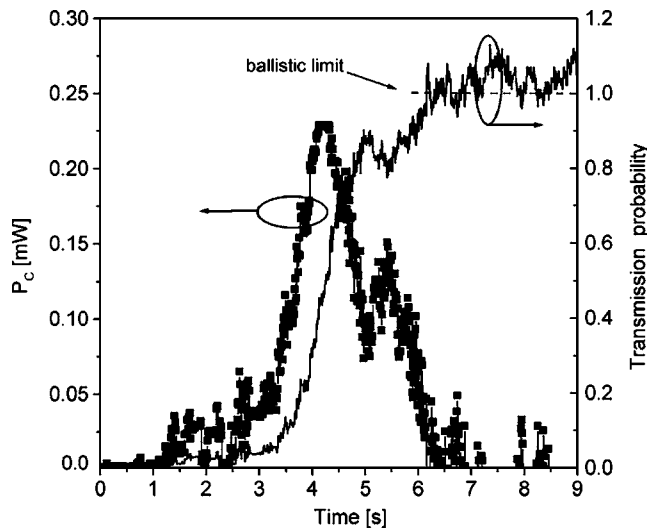


FIG. 4. Evolution of the power dissipated at the PBD constriction. Notice that as the transmission probability T (solid line) approaches unity, the power dissipation inside the constriction P_C (filled squares) decreases. For ballistic conduction ($T \approx 1$), P_C is practically negligible.

that V_C differs from V_{ox} because of the mismatch in the number of electron states at the two ends of the constriction.⁶ The evolution of P_C is shown in Fig. 4. Initially, Joule heating increases because of the growth of the spot area, which in turn lowers the tunneling barrier height. This corresponds to the SBD-HBD transition, as depicted in Fig. 3(b). However, notice that as \tilde{T} approaches unity, the dissipated power inside the constriction starts to decrease and eventually become negligible. Under this circumstance, the BD path behaves as a ballistic conductor and the power is totally dissipated at the capacitor electrodes. From a classical viewpoint, this situation closely resembles to what happens in a vacuum diode where power is dissipated at the metal plates and not in the vacuum. This power transfer can explain why a so small conducting channel is able to sustain a large stable current far from thermodynamic equilibrium conditions. Moreover, this localized heating might explain the formation of hillocks at the Si substrate during PBD.⁸ Electromigration effects within the BD path are also likely.⁹ The incorporation of these phenomena into the proposed model could lead to more complex dynamics such as the asymmetric logistic growth¹⁰ and the nonsaturating behavior of the current for prolonged injection.¹¹ These effects were not included in the present analysis.

To conclude, let us mention that the problem of power dissipation in a QPC has raised some interesting questions. As stated by Eq. (2), even in the case of ballistic conduction, the BD path has associated a finite conductance as a consequence of the contact resistances at the two ends of the constriction.⁶ During the transient, the BD spot must dissipate electrical energy at a rate $P = I_{BD} V_{ox}$ by means of some mechanism in which the energy gained by the injected electrons is passed incoherently in part to the contacts and in part

to the surroundings of the PBD path.¹² However, dissipation in a QPC is not only due to the presence of phonons but dissipation can be locally enhanced by the confinement effect. In this regard, a recent study based on the boosted Fermi function indicates that a localized elastic scattering barrier may induce dissipation by modifying the electron-phonon coupling.¹³ Nevertheless, this is at variance with earlier proposals in which dissipation is assumed to be strictly restricted to the electrodes, where strong scattering events are supposed to occur.¹⁴ Additionally, it is worth pointing out that conductance deviations from the ideally ballistic Landauer limit, as that exhibited by curve C3 in Fig. 1, are not unusual in the field of mesoscopic conductors.¹⁵ Deviations are often represented in terms of histograms and have been attributed to enhanced role of inelastic scattering within the constriction.¹⁶ This effect cannot be ruled out in our system.

In summary, we have presented a possible scenario for the PBD dynamics in ultrathin SiO₂ layers. This new approach is different from our own previous phenomenological model for the gate current based on the Verhulst equation.⁵ Here, we were able to isolate the electrical behavior of the breakdown site and relate its degradation dynamics to power dissipation. Of course, because of the many oversimplifications involved, the model has its limitations and does not attempt to cover all cases. It only suggests a new framework for the understanding and discussion of the physics associated with progressive breakdown.

This work was supported by Ministerio de Ciencia y Tecnología (Spain) under Project No. TEC2006-13731-C02-01.

¹S. Lombardo, J. Stathis, B. Linder, K. Pey, F. Palumbo, and C. Tung, *J. Appl. Phys.* **98**, 121301 (2005).

²E. Miranda, J. Suñé, R. Rodríguez, M. Nafía, X. Aymerich, L. Fonseca, and F. Campabadal, *IEEE Trans. Electron Devices* **47**, 82 (2000).

³F. Monsieur, E. Vincent, D. Roy, S. Bruyere, J. C. Vildeuil, G. Pananakakis, and G. Ghibaudo, *IEEE Int. Reliab. Phys. Symp. Proc.* **45** (2002).

⁴E. Miranda and J. Suñé, *Microelectron. Reliab.* **44**, 1 (2004).

⁵E. Miranda and A. Cester, *IEEE Electron Device Lett.* **24**, 604 (2003).

⁶S. Datta, *Electronic Transport in Mesoscopic Systems* (Cambridge University Press, Cambridge, 1998), 3, 69.

⁷A. Cester, L. Bandiera, J. Suñé, L. Boschiero, G. Ghidini, and A. Paccagnella, *Tech. Dig. - Int. Electron Devices Meet.* **2001**, 13.6.1.

⁸C. Tung, K. Pey, L. Tang, M. Radhakrishnan, W. Lin, F. Palumbo, and S. Lombardo, *Appl. Phys. Lett.* **83**, 2223 (2003).

⁹L. Zhang, Y. Mitani, and H. Satake, *IEEE Trans. Device Mater. Reliab.* **6**, 277 (2006).

¹⁰F. Palumbo, E. Miranda, and S. Lombardo, *Microelectron. Eng.* **80**, 166 (2005).

¹¹B. Kaczer, R. Degraeve, R. O'Connor, P. Roussel, and G. Groeseneken, *Tech. Dig. - Int. Electron Devices Meet.* **2004**, 713.

¹²M. Das and F. Green, *J. Phys.: Condens. Matter* **17**, V13 (2005).

¹³B. Sorée, W. Magnus, and W. Schoenmaker, *Phys. Lett. A* **310**, 322 (2003).

¹⁴S. Ulreich and W. Zwerger, *Superlattices Microstruct.* **23**, 719 (1998).

¹⁵B. Ludoph and J. van Ruitenbeek, *Phys. Rev. B* **61**, 2273 (2000).

¹⁶M. Das and F. Green, *J. Phys.: Condens. Matter* **15**, L687 (2003).